Computational Materials Science 95 (2014) 371–376

Contents lists available at ScienceDirect

Computational Materials Science

journal homepage: www.elsevier.com/locate/commatsci

# Dynamical and dielectric properties of $MP_2O_7$ (M = Ti, Zr, and Hf): A first-principles investigation

Huimin Xiang, Zhihai Feng, Yanchun Zhou *

*Science and Technology on Advanced Functional Composite Laboratory, Aerospace Research Institute of Materials and Processing Technology, No. 1 South Dahongmen Road, Beijing 100076, China*

ARTICLE INFO

*Article history:*
Received 15 May 2014
Received in revised form 29 July 2014
Accepted 31 July 2014
Available online 23 August 2014

*Keywords:*
Ceramic
Pyrophosphate
Vibrational property
Dielectric property
First principles calculation

ABSTRACT

A first-principles investigation on the structural and vibrational properties of $MP_2O_7$ (M = Ti, Zr and Hf) has been performed. Using density functional perturbation theory, the Born effective charge tensors, the IR-active phonon frequencies at the center of the Brillouin zone, and the dielectric constants of $MP_2O_7$ are obtained. Due to the complex structure of $MP_2O_7$, the Born effective charge tensors are quite complex. The anomalously large values of $Z^*$ implies the covalent bonding nature of $MP_2O_7$. The frequencies of zone center IR-active modes are closely related to the local structural and chemical environments of atoms. The electronic and static dielectric permittivities are analyzed in detail. The theoretical results highlight the vital role of $MO_6$ octahedron underpinning the properties of $MP_2O_7$.



## 1. Introduction

Low or negative thermal expansion (NTE) is relatively unusual and has led to great interest in such materials both from an academic and industrial perspective [1]. Among them, $M^{IV}A_2^VO_7$ materials have attracted much recent attentions for their isotropic low or negative thermal expansions, which could avoid the formation of microcracks as temperature changes [2]. The unusual properties of $M^{IV}A_2^VO_7$ materials originated from their complex and diverse crystal structures. At high temperatures, they tend to form simple cubic structure crystallizing in the space group $Pa\bar{3}$, which could be considered as being constructed based on a face centered cubic NaCl structure, with M atoms on the Na sites, and the bridging O atoms of the $A_2O_7$ units on the Cl sites, as shown in Fig. 1. However, at low temperatures $MA_2O_7$ materials often show significantly more complex structures since the linear A–O–A bond angles, constrained by the symmetry, are energetically unfavorable [3]. Several of these compounds have been shown to have a $3 \times 3 \times 3$ ($Z = 108$) superstructure at room temperature [4,5].

Served as a structure analogue for the other compounds, $ZrP_2O_7$ also undergoes a superstructure-subcell transition as temperature increases [6]. The diversity of the structures endues $ZrP_2O_7$ with fascinating combination of properties. It has high positive thermal expansion ($12.4 \times 10^{-6}\,K^{-1}$) from room temperature (RT) to 290 °C, followed by an intermediate thermal expansion ($5.4 \times 10^{-6}\,K^{-1}$) up to 500 °C [6]. It is a good luminescent material and a host material for rare-earth activators [7,8]. It is also considered as a promising catalyst, a catalyst support [9], and a potential electrolyte candidate for fuel cell [10]. Recently, $ZrP_2O_7$ is used as a binder in the sintering of $Si_3N_4$ ceramic and these composites could be used as a radome material because of their good mechanical and dielectric properties [11].

As a binder material, the mechanical and dielectric property of $ZrP_2O_7$ greatly affects the performance of the composites. However, few studies have been conducted focusing on the dielectric property of $ZrP_2O_7$. Kim and Yim [12] examined the dielectric constant and relaxation of $ZrP_2O_7$ and $TiP_2O_7$. They found that the polarizability of the tetravalent metal cation was one of the important factors determining the magnitude of the dielectric constant, the loss, and the dielectric stability and their dependence on temperature and frequency. However, the relationship between structure, chemistry, and dielectric properties has not been uncovered in their work. As demonstrated previously, the structure has great effects on the properties of a material [13–15]. Thus, understanding the relationship between structural and dielectric properties of $ZrP_2O_7$ is crucial to design new dielectric materials with tunable properties. In this work, first-principles calculations were performed on the dielectric properties of $MP_2O_7$ (M = Ti, Zr, and Hf). The crystal structure, Born effective charge tensors, frequencies of zone-center IR-active modes and static dielectric permittivity were calculated. The characteristics of crystal structure and bonding of $MP_2O_7$ were examined and their effects on dynamical and

* Corresponding author. Tel.: +86 10 6838 2478; fax: +86 10 6875 9874.
*E-mail addresses:* yczhou714@gmail.com, yczhou@imr.ac.cn (Y. Zhou).

http://dx.doi.org/10.1016/j.commatsci.2014.07.054
0927-0256/

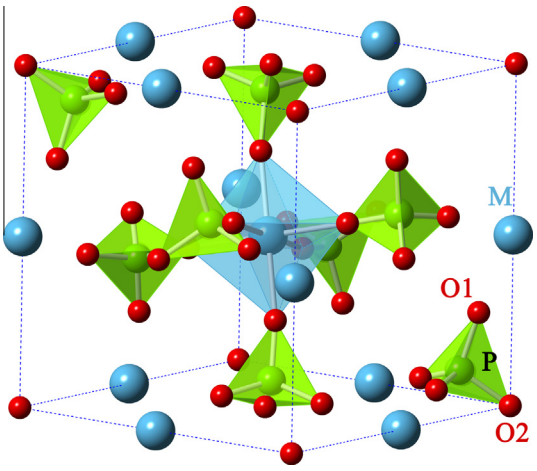


**Fig. 1.** Crystal structure of ideal parent structure of $MP_2O_7$.

dielectric properties were revealed. Our results highlight the vital role of $MO_6$ octahedron on the dielectric permittivity of $MP_2O_7$.

## 2. Computational methods

The first-principles calculations were performed using the Cambridge Serial Total Energy Package (CASTEP) code [16] based on density functional theory (DFT). Norm-conserving pseudopotentials [17] were employed throughout this work to describe the ion–electron interactions for Ti, Zr, Hf, P and O atoms. The electronic exchange–correlation energy was treated under local density approximation (LDA) [18]. The plane-wave basis set cutoff was 850 eV for all calculations. The special *k*-points sampling integration over the Brillouin zone was employed by using the Monkhorst–Pack method with a $2 \times 2 \times 2$ special *k*-point mesh [19]. These parameters were sufficient in leading to well-converged total energies and geometrical configurations. Increasing the plane-wave cutoff energy and the *k*-point mesh to 1000 eV and $6 \times 6 \times 6$ only led to changes in total energy by less than 0.003 eV · atom$^{-1}$ and the lattice constant by less than 0.01%. The crystal structures of $MP_2O_7$ were fully optimized by independently modifying lattice constant and internal atomic coordinates under the Broyden–Fletcher–Goldfarb–Shanno (BFGS) minimization scheme [20]. The tolerances for geometrical optimization were: differences for total energy within $5 \times 10^{-6}$ eV/atom, maximum ionic Hellmann–Feynman force within 0.01 eV/Å, maximum ionic displacement within $5 \times 10^{-4}$ Å, and maximum stress within 0.02 GPa.

The vibrational frequencies at the *G* point, the transverse optical–longitudinal optical (TO–LO) splitting of the zone-center optical modes and dielectric properties were calculated using the density functional perturbation theory [21,22]. The dynamical matrix, phonons and dielectric response are obtained as second derivative of the total energy with respect to a given perturbation in ionic positions or an external electric field. The TO–LO splitting of $MP_2O_7$ are obtained by introducing the non-analytic term to the dynamical matrix.

## 3. Results and discussions

### 3.1. Structure of $MP_2O_7$

The ideal parent structure of $MP_2O_7$ which crystallized in a $Pa\bar{3}$ space group is comprised by two basic units: octahedrally bonded M metal, and tetrahedrally bonded phosphate groups. Each $MO_6$ octahedron shares its corners with six tetrahedra and each tetrahedron shares three of its corners with three octahedra and the remaining corner with another tetrahedron. The unit cell of $MP_2O_7$ contains four formula units ($Z = 4$), as shown in Fig. 1. Note that there are two nonequivalent oxygen sites: bridging oxygen atoms between $MO_6$ and $PO_4$ units and bridging oxygen atoms of $P_2O_7$ units. Here, we labeled the former as O1, and the latter as O2. The positions of the M and O2 atoms are imposed by symmetry: they are located at (0.5, 0.5, 0.5) and (0, 0, 0) on the 4*b* and 4*a* Wyckoff sites, respectively. The P atoms occupy the 8*c* Wyckoff site (*m*, *m*, *m*), and O1 atoms occupy the 24*d* Wyckoff site (*u*, *v*, *w*), where *m*, *u*, *v* and *w* are internal parameters.

**Table 1**
Calculated and experimental lattice parameters of $MP_2O_7$.

| | $TiP_2O_7$ | | $ZrP_2O_7$ | | $HfP_2O_7$ | |
|---|---|---|---|---|---|---|
| | Cal. | Exp.[20] | Cal. | Exp.[21] | Cal. | Exp.[22] |
| *a* (Å) | 8.0706 | 7.879 | 8.4182 | 8.2899 | 8.2853 | 8.2147 |
| *m* | 0.1103 | | 0.1067 | 0.1054 | 0.1073 | |
| *u* | 0.0593 | | 0.0575 | 0.0550 | 0.0582 | |
| *v* | 0.2838 | | 0.2751 | 0.2733 | 0.2761 | |
| *w* | 0.0797 | | 0.0769 | 0.0760 | 0.0763 | |

The completely relaxed structural parameters for three compounds under LDA are tabulated in Table 1, together with the experimental lattice constants previously reported [23–25] for comparisons. The overall agreements are satisfactory. The calculated lattice constants deviated from the experimental data within 0.9%, 1.5% and 2.4% for $HfP_2O_7$, $ZrP_2O_7$ and $TiP_2O_7$, respectively. The very close agreement with the experimental results provides a good confirmation of the reliability of our calculations.

The calculated Mulliken populations, bond lengths and all possible bond angles for $MP_2O_7$ are listed in Table 2. The previously reported experimental data [24] for $ZrP_2O_7$ are also included for comparisons. Our theoretical results for $ZrP_2O_7$ are quite coincident with the experimental data. In all these compounds, interestingly, the structure of $PO_4$ groups remains unchanged, the Mulliken populations and bond lengths of P–O1 and P–O2 are nearly the same. Obviously, the impact of variation in M atom on the structure of $PO_4$ groups is quite limited. It is also notable that the bond lengths and Mulliken populations of P–O1 and P–O2 bonds are quite different from each other in all these compounds. Compared with P–O1 bonds, the lengths of P–O2 bonds are longer, while the Mulliken populations are smaller. Meanwhile, the bond angles of $PO_4$ groups deviate from the value in regular tetrahedra, 109.5°. The diversities of the Mulliken populations and the O–P–O bond angles illustrate the distortion of $PO_4$ tetrahedra in these materials, and the P atoms deviate from the center of $PO_4$ tetrahedra. In other words, the chemical environment of P atoms is complex for all these compounds. The length of M–O1 bonds shrinks from 2.074 to 1.920 Å in the order of Zr–O1, Hf–O1 and Ti–O1 since the radius of octahedrally bonded ion decreased in the order of $Zr^{4+}$ (72 pm), $Hf^{4+}$ (71 pm) and $Ti^{4+}$ (61 pm) [26]. In general, the chemical environments for P, O and M atoms are quite complex in $MP_2O_7$, which suggests that the contributions of different atoms to the vibrational and dielectric properties are complex. This is manifest from the Born effective charge tensors for P, O and M atoms in the next section.

### 3.2. Born effective charge tensors

The Born effective charge (BEC) tensors $Z^*_{\kappa,ij}$ is a fundamental quantity for the study of lattice dynamics, controlling the long-range Coulomb part of the force constants. They are defined as the proportionality coefficient relating, at linear order, to the polarization per unit cell, created along the direction *i*, and the displacement along the direction *j* of the atoms belonging to the sub-lattice $\kappa$, under the condition of a zero electric field [22]. They are quite